GEOPHYSICAL RESEARCH LETTERS, VOL. 35, L06402, doi:10.1029/2007GL032865, 2008

Electrowetting on mineral and rock surfaces

F. M. Francisca,[1] D. Fratta,[2] and H. F. Wang[3]

Received 3 December 2007; revised 5 February 2008; accepted 18 February 2008; published 20 March 2008.

[1] Electrowetting was investigated as a method to influence fluid movement on mineral or rock surfaces. The experimental setup was to place a small drop of water containing an electrolyte on a solid surface directly or on the same solid surface coated with a hydrophobic film. The contact angle decreased with an applied electric field until it reached a saturation value associated with a critical voltage. The electrowetting experiments were conducted again after surfactant was added to the water drop. In all cases the contact angle decreased with increasing voltage and surfactant concentration. Electrowetting enhanced the wetting effect over that of the surfactant alone both by lowering the contact angle and by promoting rupture of the hydrophobic film. Four zones of behavior were identified based on the surfactant concentration and the voltage level. The results open the possibility that electrowetting can be used to enhance mobilization of one fluid relative to another in hydrocarbon recovery or contaminant remediation, as interfacial tensions control multiphase fluid flow. **Citation:** Francisca, F. M., D. Fratta, and H. F. Wang (2008), Electrowetting on mineral and rock surfaces, *Geophys. Res. Lett.*, *35*, L06402, doi:10.1029/2007GL032865.

1. Introduction

[2] In the past several decades, many techniques have been proposed and implemented to enhance oil recovery and increase the efficiency of decontamination processes [*Lake*, 1989; *Sahimi*, 1993]. Recovery and remediation techniques include the injection of high pressure fluid, steam or gas, or the addition of bacteria, brine or surface-active agents to promote immiscible fluid displacement [*Finnerty and Singer*, 1983; *Stokes et al.*, 1986; *Pennell et al.*, 1993; *Wasan and Nikolov*, 2003]. For a given pore structure and fluid pressure, the detachment, mobilization, and displacement of trapped oil depends on the contact angle and the interfacial tension [*Stokes et al.*, 1986; *Adamson and Gast*, 1997].

[3] Interfacial tensions determine the shape of macroscopic drops of liquids in contact with a solid flat surface. At equilibrium, the drop satisfies the following condition (Figure 1a; Young model):

$$\cos(\theta_0) = \frac{\gamma_{SV} - \gamma^0_{SL}}{\gamma_{LV}} \tag{1}$$

where θ_0 is the initial liquid-vapor and solid surface contact angle, γ^0_{SL} is the intrinsic solid-liquid interfacial tension, γ_{LV} is the liquid-vapor interfacial tension and γ_{SV} is the solid-vapor interfacial tension. The wetted part of the solid substrate is delimited by a contact line along which the three phases are in contact. The final shape of the drop depends on the interaction between the free energy change needed to expand the area of each interface and the physical-chemical interaction between phases. As a result, θ_0 is a measure of the ability of each fluid phase to wet the solid surface.

[4] Any interacting chemical or physical effect capable of modifying interfacial tensions induces changes in θ_0 (e.g., adding surfactants or increasing the fluid temperature [*Adamson and Gast*, 1997]). Decreasing the solid-liquid interfacial tension γ_{SL} favors the displacement of the contact line and the liquid-gas interface [*Finnerty and Singer*, 1983]. The same principle applies for any two immiscible liquid phases in physical-chemical equilibrium. Of special interest to us is that the physical-chemical equilibrium is altered by applying an electric field between the solid and an electrolyte [*Verjheijen and Prins*, 1999; *Prins et al.*, 2001; *Quillet and Berge*, 2001]. Accumulation of hydrated ions at the liquid-solid interface reduces interfacial tension [*Lippmann*, 1875; *Rosslee and Abbott*, 2000] and promotes the rupture of hydrocarbon films coating mineral surfaces [*Sharma and Reiter*, 1996]. The wetting of a dielectric solid surface is favored because γ_{SL} is lowered according to the equation [*Mugele and Baret*, 2005; *Berry et al.*, 2006]:

$$\gamma_{\mathrm{SL}} = \gamma^0_{\mathrm{SL}} - \frac{1}{2}\mathrm{C}\,\mathrm{V}^2 \tag{2}$$

where $C = \varepsilon_o \cdot \varepsilon/d$ is the capacitance per unit area, ε_o is the permittivity of vacuum, ε is the relative static permittivity of the solid phase, d is the dielectric thickness, and V is the applied voltage. Because of the influence of V on γ_{SL}, the size of the wetted area increases leading to a new equilibrium position and contact angle θ (Figure 1b; Lippmann-Young model [*Mugele and Baret*, 2005; *Berry et al.*, 2006]):

$$\cos(\theta) = \cos(\theta_0) + \frac{\varepsilon_0\,\varepsilon\,\mathrm{V}^2}{2\,\gamma_{\mathrm{LV}}\,\mathrm{d}} \tag{3}$$

[5] This phenomenon, known as electrowetting, is independent of ionic concentration [*Verjheijen and Prins*, 1999; *Kuo et al.*, 2003] but can only reduce θ to a voltage-saturated value [*Peykov et al.*, 2000; *Mugele and Baret*, 2005]. This saturation of the contact angle, which is sometimes explained by the ionization of the non-wetting fluid at the contact line [*Vallet et al.*, 1999] or by the non-perfect dielectric behavior of solids [*Shapiro et al.*, 2003],

[1]Universidad Nacional de Córdoba and Consejo Nacional de Investigaciones Científicas y Técnicas (CONICET), Córdoba, Argentina.
[2]Geological Engineering Program, University of Wisconsin-Madison, Madison, Wisconsin, USA.
[3]Geology and Geophysics, University of Wisconsin-Madison, Madison, Wisconsin, USA.

0094-8276/08/2007GL032865$05.00

takes place at the critical voltage (V_{crit}) [*Quinn et al.*, 2005]:

$$V_{crit}^2 = 2d\frac{\gamma_{SV} - \gamma_{LV}\cos(\theta_0)}{\varepsilon_0\varepsilon} \quad (4)$$

[6] Here we show that the wettability [*de Gennes*, 1985; *Morrow*, 1990] of mineral and rock surfaces can be significantly enhanced by the process of electrowetting [*Verjheijen and Prins*, 1999; *Quillet and Berge*, 2001; *Kang*, 2002; *Hayes and Feenstra*, 2003; *Kuo et al.*, 2003; *Shapiro et al.*, 2003; *Mugele and Baret*, 2005]. We demonstrate that the combined contribution of electrowetting and detergents reduces contact angle by an additional 24% over the value obtained using surface-active agents alone. These results provide a new conceptual methodology for the improved removal of petroleum hydrocarbons from mineral surfaces.

2. Methods

[7] Thin sections were prepared from six mineral (quartz, calcite, barite, plagioclase, talc, and hematite) and six rock (marble, gneiss, granite, basalt, shale, and limestone) specimens and glued to a glass slide covered with a thin film of conductive silver paint (Figure 1). The final thicknesses and surfaces were obtained by polishing the specimens with 6 mm silicon carbide grinding wheels. Before testing, all specimens were washed with deionized water, oven dried until achieving a constant weight, and then kept at room temperature for 24 hrs. Each thin section was placed on a horizontal surface with the testing surface facing up. A drop of one of three different electrolytes was placed on the testing surface with a calibrated micropipette. The two electrodes were connected to a 313A Bertan high voltage DC power supply. The electrolyte drop geometry was documented with a 480 × 640-pixel digital camera and the contact angle was obtained using digital image processing. The right and left angles formed by the tangent line to the drop and the solid surface were obtained by means of an image analysis algorithm and verified manually. The initial contact angle was measured after a period of stabilization of 4 min. Some specimens were coated with a hydrophobic film to analyze the effect of voltage on film rupture and wettability. All specimen surfaces were examined under a Fisher Scientific Stereomaster microscope (magnification 20 to 40×) in order to verify the film rupture after testing.

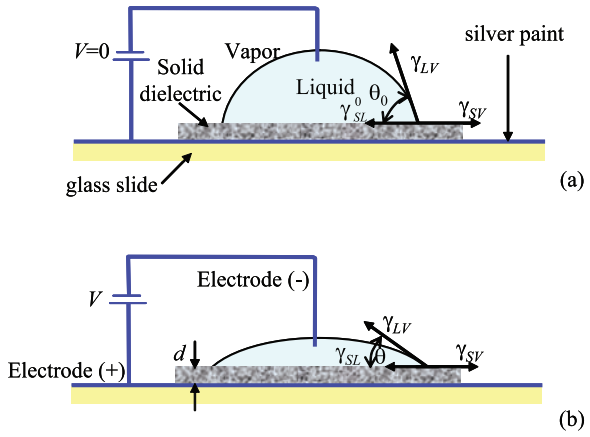

Figure 1. Equilibrium position for sessile drops. (a) Young contact angle; (b) Lippmann-Young contact angle and principle of electrowetting. The two electrodes are the conductive silver paint under the solid dielectric and the stainless steel wire connected to the fluid drop. The wire diameter is 0.64 mm.

3. Results

[8] Here, we focus on phase interactions of electrolytes with natural mineral and rock surfaces with the goal of increasing the wetting of these materials. Figure 2 shows the influence of V on the normalized change of $\cos(\theta)$ for three different electrolytes over a limestone surface. A good agreement with equation (3) is observed. The increasing deviation between the model response and the experimental data at electrical potentials lower than −200V and higher than +200 V corresponds to the voltage saturation of the contact angle.

[9] No significant asymmetry is observed when the polarity of the electrodes is reversed (Figure 1b). In this case, the negatively charged Cl^- ions move toward the steel wire, while Na^+ and Mg^{2+} ions move toward the solid surface. The radii of these hydrated ions are: Cl^- = 0.332 nm, Na^+ = 0.358 nm, and Mg^{2+} = 0.476 nm. We observed (Figure 2) little effect of valence or hydrated size of the ions on the saturated value of the contact angle, about a 15% increase over $\cos(\theta_0)$.

[10] We next conducted a series of experiments of wettability on a hydrophobic surface. Pure mineral and rock surfaces were coated with petrolatum gel (i.e., commercially

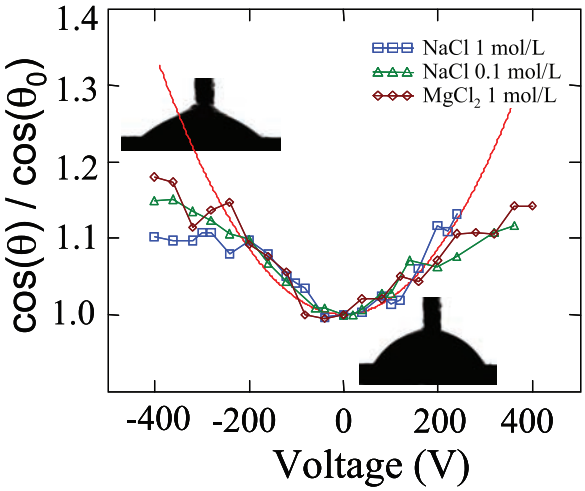

Figure 2. Electrowetting phenomenon on a limestone surface. Influence of voltage on the relative change of contact angles for drops of 0.1 mol/L and 1.0 mol/L NaCl and 1.0 mol/L $MgCl_2$ solutions. The solid line shows the expected behavior according to the Lippmann-Young model. The limestone thickness is 400 μm and the limestone relative static permittivity is 7.3. Positive and negative voltages were tested on different electrolytes drops. Similar trends were observed on calcite, barite, and marble specimens.

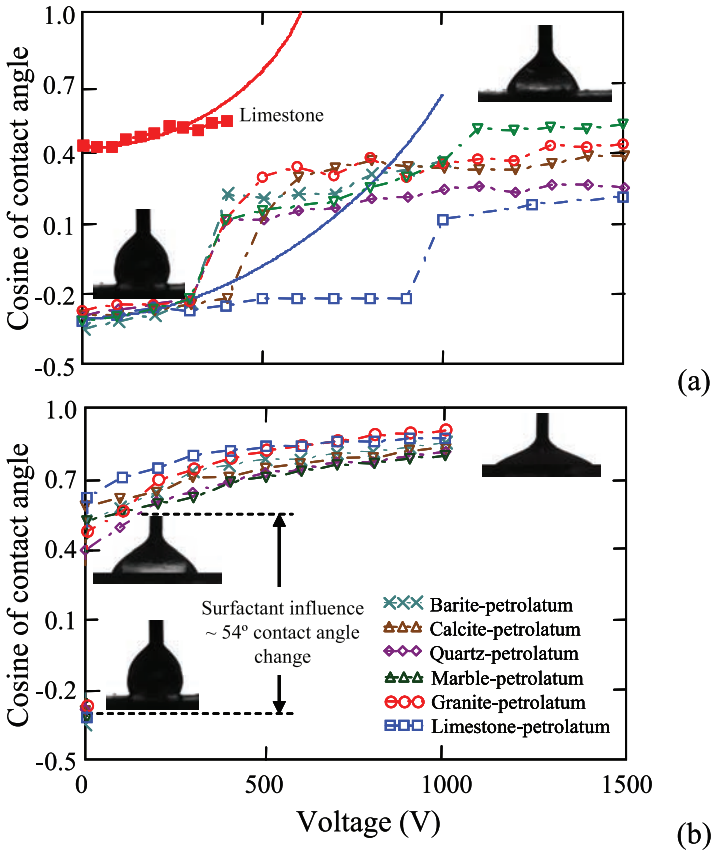

Figure 3. Wetting changes induced by the applied electric field: influence of the applied voltage on cos(θ) for mineral and rock specimens coated with a petrolatum film. The petrolatum consists of non-polar iso- and cyclo-paraffins with some alkylated aromatic hydrocarbons. The film thickness is approximately 10 μm and the mineral and rock thicknesses are 400 μm. The solid lines show the behavior predicted by the Lippmann-Young model. The initial θ measured before the application of the petrolatum film were 59.5°, 55.1°, 15.1°, 57.9°, 10.8°, and 59.0° for the barite, calcite, quartz, marble, granite, and limestone specimens, respectively. The volume of the drops shown in the pictures is 4 μL. The coefficient of variation for the measured θ is 3%. (a) Without surfactant: Drops are a 0.1 mol/L NaCl solution (The experimental data and the model response for the limestone specimen without the petrolatum film is shown as a reference behavior for untreated surfaces); (b) With surfactant: The liquid drop is a 0.1 mol/L NaCl solution with 2% w/w of detergent (a coconut-based anionic surfactant – "alcohols, (C12–14), ethoxylated, monoethers with sulphuric acid, and sodium salts").

available petroleum jelly) rendering hydrophobic specimens ($\theta_0 \approx 106.9°$). We observed that the initial contact angles remained constant with time and no changes in the hydrophobic film were detected (specimens were observed for 15 min under a microscope in order to verify equilibrium conditions). In Figure 3a electrowetting is responsible for the continuous reduction of θ at low voltages. When electric potentials in the 400–500 V range, or 900 V in the case of limestone, were applied, we observed a sharp increase in cos(θ) to values higher than those predicted by equation (3). The step changes are associated with rupture of the hydrophobic film caused by the electrical attraction of hydrated ions toward the dielectric surface, which reduces θ and causes an enlargement of the wetted solid surface [*Hayes and Feenstra*, 2003]. The rupture of the hydrophobic film was confirmed by observing the specimens under a microscope. The observed gaps show how the electrolyte liquid reaches the contaminated solid surface and solid-fluid-petrolatum contact lines develop. The higher voltage required for limestone can be attributed to a relatively high attraction between this material and the film [*Basu and Sharma*, 1996; *Sharma and Reiter*, 1996; *Bergeron*, 1999] and to the smoothness of the limestone surface with an absence of discontinuities (as observed under the microscope). Above the rupture voltage cos(θ) increases slowly toward an asymptotic value as voltage increases.

[11] A surfactant decreases γ_{SL} and γ_{LV} therefore reducing the macroscopic contact angle (when the concentration is lower than the critical micelle concentration – CMC [*Adamson and Gast*, 1997]). We found that cos(θ) at 0V increases from −0.3 to the +0.5 to +0.7 range in all petrolatum-covered mineral and rock specimens when a detergent is added to the electrolyte (Figure 3b), Also, the film ruptures a few seconds after the fluid drop is placed on the petrolatum film and the contact line needs almost 4 minutes to reach a new equilibrium position. Thereafter, a small electrowetting increase in cos(θ) of ~0.1 is observed as V increases, which is likely produced by the accumulation of electrical charges near the solid surface and the

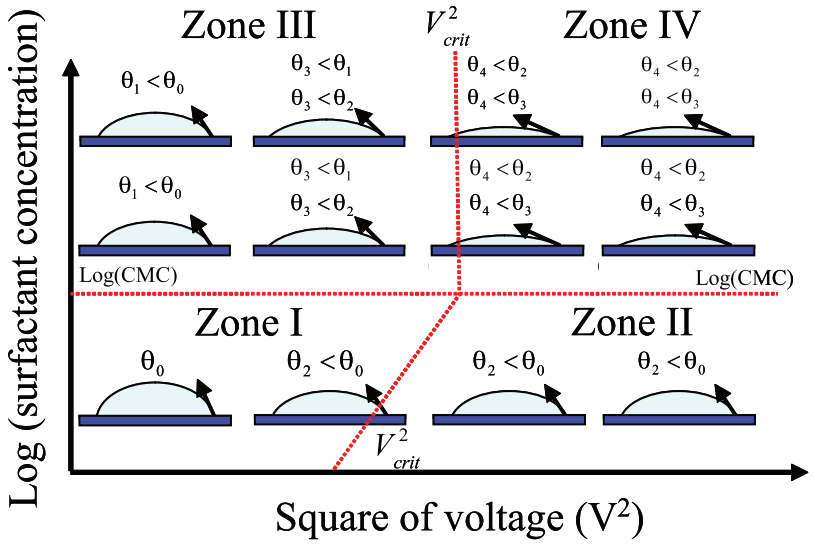

Figure 4. Schematic illustration of the simultaneous effect of surfactant and electrowetting on θ. The relative importance of voltage and surfactant is determined from the change in the contact angle. The region boundaries are established by the electrowetting contact angle saturation voltage and the critical micelle concentration. The electrowetting contact angle saturation voltage increases with greater surfactant concentration (boundary between Zones I and II below CMC).

consequent reduction of γ_{SL} [*Lippmann*, 1875; *Verjheijen and Prins*, 1999; *Moon et al.*, 2002].

4. Discussion

[12] We first present a qualitative analysis of the simultaneous effect of surfactant and electrowetting on the contact angle (Figure 4). Based on over one hundred experimental runs, we identified four different zones with distinctive behavior. The region boundaries are established by the electrowetting contact angle saturation voltage [*Quinn et al.*, 2005] and the critical micelle concentration - CMC [*Adamson and Gast*, 1997]. *Zone I*: Low voltage ($V < V_{crit}$) and low surfactant concentration, C < CMC: θ is reduced by increasing the applied voltage or the surfactant concentration. *Zone II*: $V > V_{crit}$, C < CMC: only the addition of surfactants can enhance the wetting of solid surfaces. *Zone III:* $V < V_{crit}$, C > CMC: θ is only susceptible to voltage changes. *Zone IV*: $V > V_{crit}$, C > CMC: no further reduction in θ is possible. The slope of the Zone I and Zone II boundary shows the effect of the two contributing phenomena. At surfactant concentrations less than CMC, the surfactant decreases both γ_{SL} and γ_{LV} reducing the macroscopic contact angle [*Adamson and Gast*, 1997], and the decrease in γ_{SL} also contributes to the reduction of θ by electrowetting and the increase in the value of V_{crit} (Equation 4 [*Quinn et al.*, 2005]). These effects cease to contribute above the CMC and the slope of the V_{crit} boundary changes as shown in Figure 4.

[13] We can recognize these four regions in the experimental results shown in Figure 3. The tests begin in zone I and move toward zone II by increasing the applied voltage and reducing θ until the contact angles reach saturation in the surfactant-free electrolyte (Figure 3a). Figure 3b shows the transition of θ from zone I to III when the fluid drop is treated with the detergent and the external electric field is zero. Thereafter, as the voltage increases, θ moves from zone III to IV after surpassing V_{crit} and become saturated at a contact angle that is the combined effect of both electrowetting saturation and critical micelle concentration.

[14] We have shown through experimental evidence that the combined contribution of electrowetting and surfactants helps to increase the wetted surface of natural mineral and rock surfaces. The measured contact angles decrease significantly due to the simultaneous contribution of electric voltage and detergent. The contact angle decreases 44.6% when electrowetting acts alone and it decreases 51.5% by the sole action of the detergent with respect to θ_0. The decrease of θ is 75.5% when the electric voltage and detergent concentrations are both increased. Hence, the additional effect due to electrowetting is equivalent to an additional decrease of 24% in the contact angle. The change in $\cos(\theta)$ caused by the electrowetting phenomenon shown in Figure 3b corresponds to an increase in the capillary pressure $\Delta p_c \propto \gamma_{LV} \cdot [\cos(\theta) - \cos(\theta_0)]$ of approximately 40%. Furthermore, the accumulation of electrical charges at the liquid-solid interfaces caused by the electrowetting phenomenon promotes the rupture of hydrocarbon films coating mineral surfaces [*Sharma and Reiter*, 1996]. These results give novel possibilities to the removal of petroleum hydrocarbons and to the wetting of mineral surfaces by electrified liquids. The combined application of electrowetting phenomena and surfactant agents could be the basis for the development of new quaternary oil recovery techniques.

[15] **Acknowledgments.** This research was supported in part by a Fulbright-CONICET Award and the University of Wisconsin-Madison.

References

Adamson, A. W., and A. P. Gast (1997), *Physical Chemistry of Surfaces*, John Wiley, New York.

Basu, S., and M. M. Sharma (1996), Measurement of critical disjoining pressure for dewetting of solid surfaces, *J. Colloid Interface Sci.*, *181*, 443–455.

Bergeron, V. (1999), Forces and structure in thin liquid soap films, *J. Phys. I*, *11*, R215–R238.

Berry, S., J. Kedzierski, and B. Abedian (2006), Low voltage electrowetting using thin fluoropolymer films, *J. Colloid Interface Sci.*, *303*, 517–524.

de Gennes, P. G. (1985), Wetting: Statics and dynamics, *Rev. Mod. Phys*, *57*, 827–863.

Finnerty, W. R., and M. E. Singer (1983), Microbial enhancement of oil recovery, *Nature Biotechnol.*, *1*, 47–54.

Hayes, R. A., and B. J. Feenstra (2003), Video-speed electronic paper based on electrowetting, *Nature*, *425*, 383–385.

Kang, K. H. (2002), How electrostatic fields change contact angle in electrowetting, *Langmuir*, *18*, 10,318–10,322.

Kuo, J. S., P. Spicar-Mihalic, I. Rodriguez, and D. T. Chiu (2003), Electrowetting-induced droplet movement in an immiscible medium, *Langmuir*, *19*, 250–255.

Lake, L. W. (1989), *Enhanced Oil Recovery*, Prentice-Hall, New York.

Lippmann, G. (1875), Relations entre les phénomènes électriques et capillaires, *Ann. Chim. Phys*, *5*, 494–549.

Moon, H., S. K. Cho, R. L. Garrell, and C. J. Kim (2002), Low voltage electrowetting-on-dielectric, *J. Appl. Phys.*, *92*, 4080–4087.

Morrow, N. R. (1990), Wettability and its effect on oil recovery, *J. Pet. Technol.*, *42*, 1476–1484.

Mugele, F., and J. C. Baret (2005), Electrowetting: From basic to applications, *J. Phys. Condens. Matter*, *17*, R705–R774.

Pennell, K. D., L. M. Abriola, and W. Weber (1993), Surfactant enhanced solubilization of residual dodecane in soil columns: 1. Experimental investigation, *Environ. Sci. Technol.*, *27*, 2332–2340.

Peykov, V., A. Quinn, and J. Ralston (2000), Electrowetting: A model for contact-angle saturation, *Colloid Polym. Sci.*, *278*, 789–793.

Prins, M. W. J., W. J. J. Welters, and J. W. Weekamp (2001), Fluid control in multichannel structures by electrocapillary pressure, *Science*, *291*, 277–280.

Quillet, C., and B. Berge (2001), Electrowetting: A recent outbreak, *Curr. Opinion Colloid Interface Sci.*, *6*, 34–39.

Quinn, A., R. Sedev, and J. Ralson (2005), Contact angle saturation in electrowetting, *J. Phys. Chem. B*, *109*, 6268–6275.

Rosslee, C., and N. L. Abbott (2000), Active control of interfacial properties, *Curr. Opinion Colloid Interface Sci.*, *5*, 81–87.

Sahimi, M. (1993), Flow phenomena in rocks: From continuum models to fractals, percolation, cellular automata, and simulated annealing, *Rev. Mod. Phys.*, *65*, 1393–1534.

Shapiro, B., H. Moon, R. L. Garrell, and C. J. Kim (2003), Equilibrium behavior of sessile drops under surface tension, applied external fields and material variations, *J. Appl. Phys.*, *93*, 5794–5811.

Sharma, A., and G. Reiter (1996), Instability of thin polymer films on coated substrates: Rupture, dewetting, and drop formation, *J. Colloid Interface Sci.*, *178*, 383–399.

Stokes, J. P., D. A. Weitz, J. P. Gollub, A. Dougherty, M. O. Robbins, P. M. Chaikin, and H. M. Lindsay (1986), Interfacial stability of immiscible displacement in a porous medium, *Phys. Rev. Lett.*, *57*, 1718–1721.

Vallet, M., M. Vallade, and B. Berge (1999), Limiting phenomena for the spreading of water on polymer films by electrowetting, *Eur. Phys. J. B*, *11*, 583–591.

Verjheijen, H. J. J., and M. W. J. Prins (1999), Reversible electrowetting and trapping charge: Model and experiments, *Langmuir*, *15*, 6616–6620.

Wasan, D. T., and A. D. Nikolov (2003), Spreading of nanofluids on solids, *Nature*, *423*, 156–159.

F. M. Francisca, Universidad Nacional de Córdoba and Consejo Nacional de Investigaciones Científicas y Técnicas (CONICET), Av. Velez Sarsfield 1611, CP 5016, Córdoba, Argentina. (ffrancis@efn.uncor.edu)

D. Fratta, Geological Engineering Program, University of Wisconsin-Madison, 1415 Engineering Drive, Madison, WI 53706, USA. (fratta@wisc.edu)

H. F. Wang, Geology and Geophysics, University of Wisconsin-Madison, 1215 W Dayton St., Madison, WI 53706, USA. (wang@geology.wisc.edu)